nature protocols

SUPPLEMENTARY INFORMATION

https://doi.org/10.1038/s41596-018-0026-5

In the format provided by the authors and unedited.

Fit-free analysis of fluorescence lifetime imaging data using the phasor approach

Suman Ranjit[1,4], Leonel Malacrida[1,2,4], David M. Jameson[3] and Enrico Gratton[1]*

[1]Laboratory for Fluorescence Dynamics, Department of Biomedical Engineering, University of California at Irvine, Irvine, CA, USA. [2]Departamento de Fisiopatología, Hospital de Clínicas, Universidad de la República, Montevideo, Uruguay. [3]Department of Cell and Molecular Biology, University of Hawaii at Manoa, Honolulu, HI, USA. [4]These authors contributed equally: Suman Ranjit, Leonel Malacrida.
*e-mail: egratton22@gmail.com

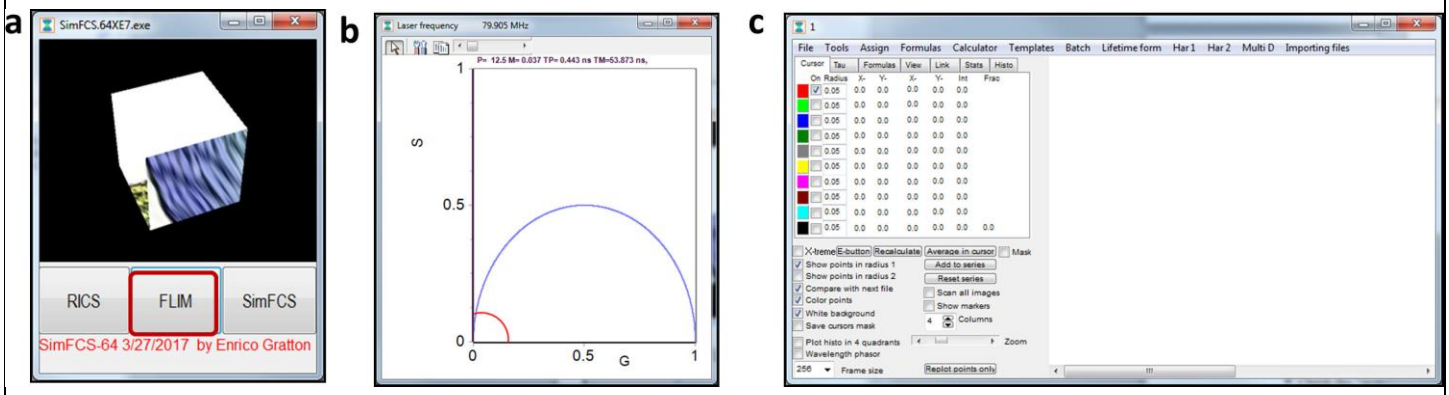

Supplementary Figure 1

Layout of SimFCS – FLIM module.

a) The front panel and the FLIM button (in red). b) Phasor plot and c) Data analysis window.

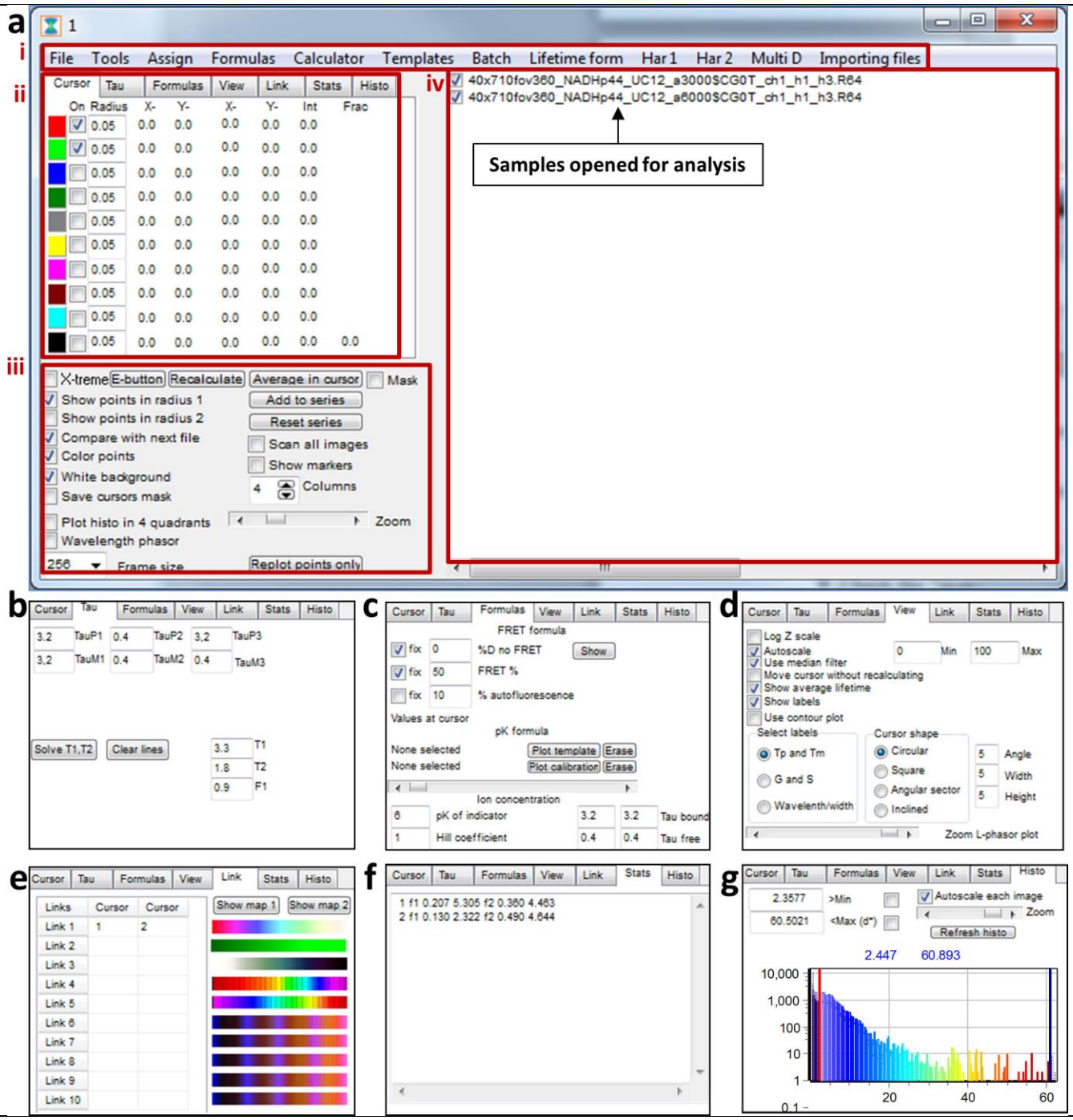

Supplementary Figure 2

SimFCS - Details of the FLIM analysis window.

a) Different parts of the analysis window. The four red options show the different parts of the analysis. b-g) Tabs from Option ii.

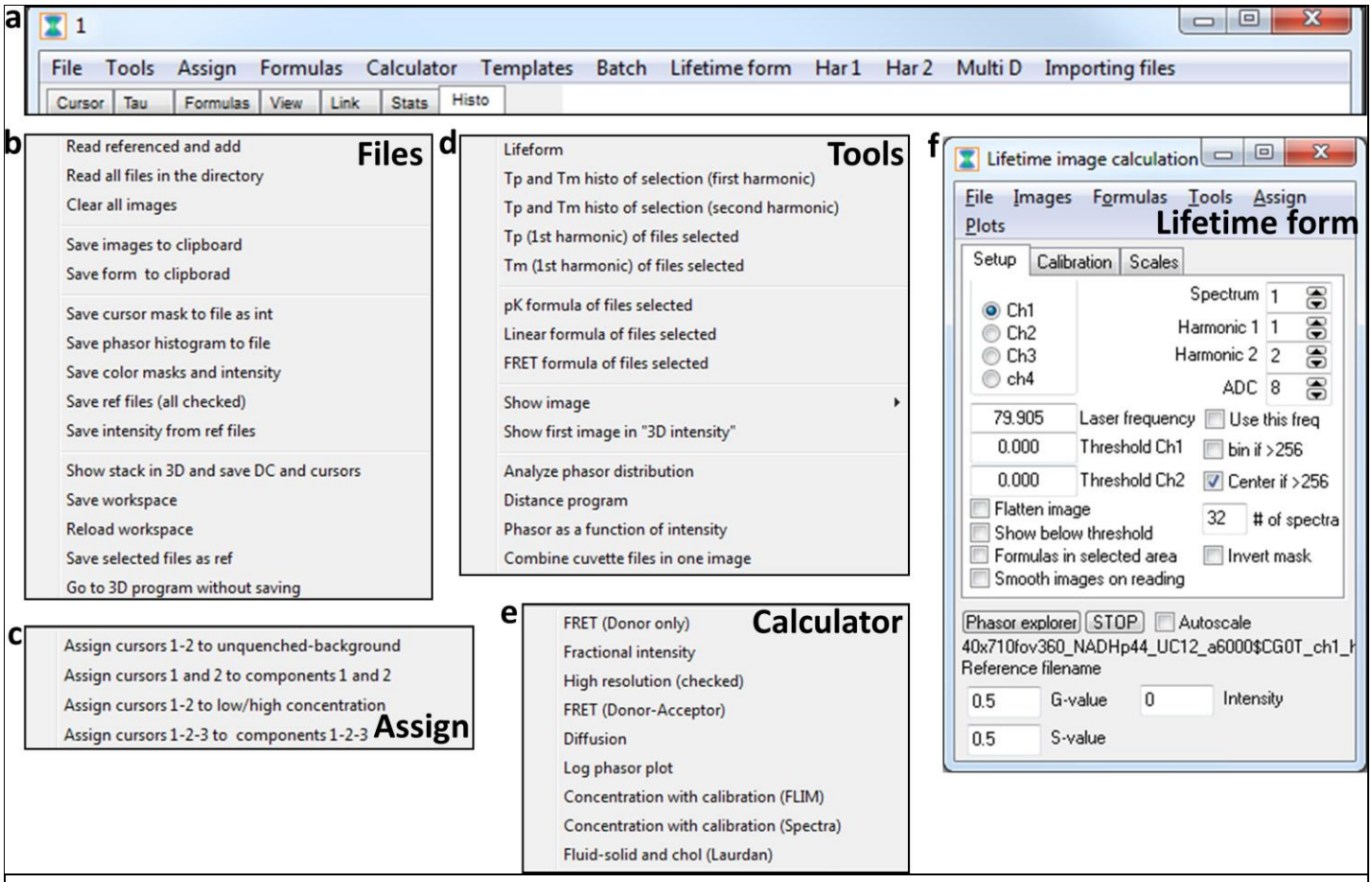

Supplementary Figure 3

Details of the FLIM analysis window – option 1 of Figure S2a

a) Different tabs associated with option 1 of analysis window. b-f) Options of different analysis in these tabs.

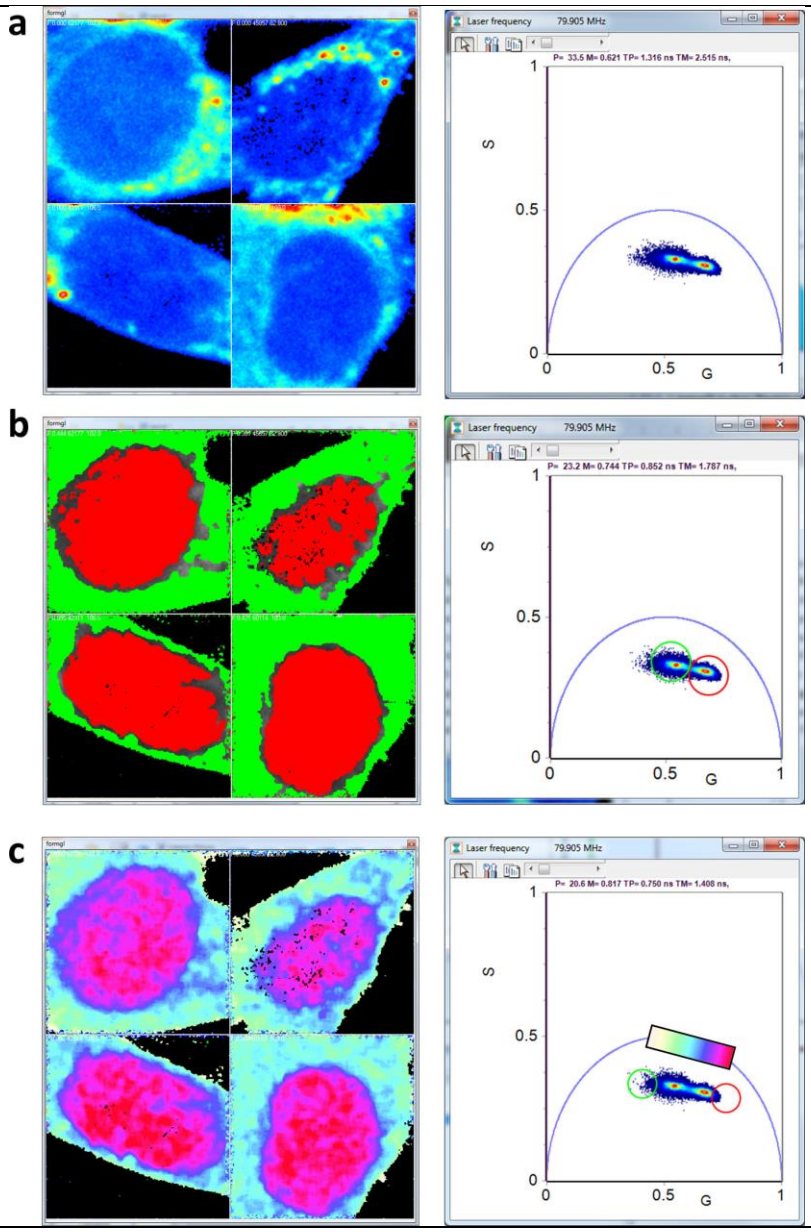

Supplementary Figure 4

Color mapping using phasor approach.

a) Background corrected autofluorescence intensity images and the corresponding phasor map. b) Two-color map of the FLIM signature using the red and green cursor in the phasor map. c) Continuous color scheme to paint the FLIM images.

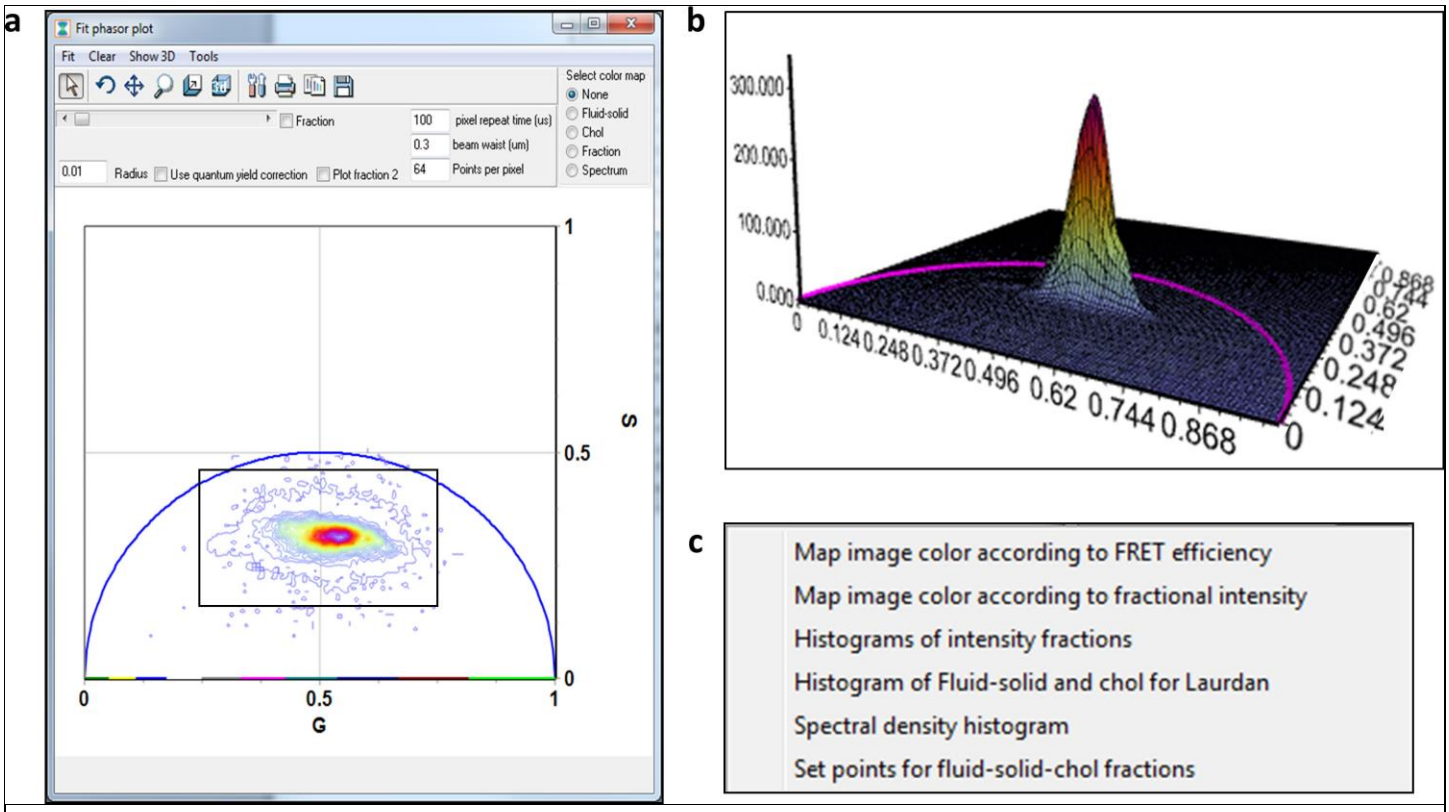

Supplementary Figure 5

Details of the 'Fractional analysis' window.

a) The high resolution phasor heat map and corresponding analysis options. b) The phasor heat map presented as the 3D plot. c) Analysis options that can be accessed using the Tools button of a.

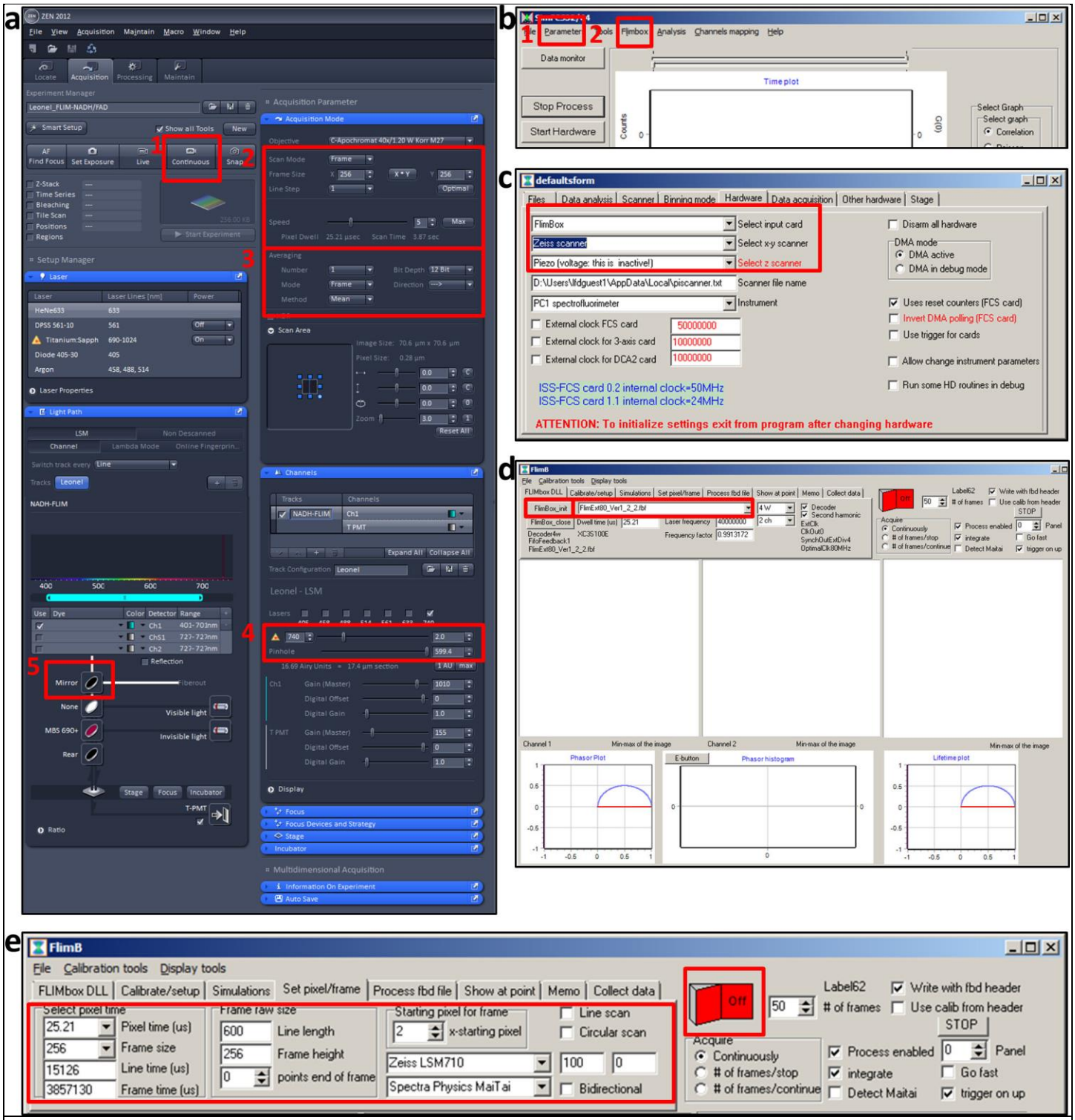

Supplementary Figure 6

FLIM acquisition – setting up FLIMbox.

a) Acquisition window of the Zeiss Zen software, b) Selection pane for the input, c) Choosing the right input scanner cards using SimFCS, d) FLIMbox window of SimFCS and e) selecting parameters to properly synchronize Zen with SimFCS.

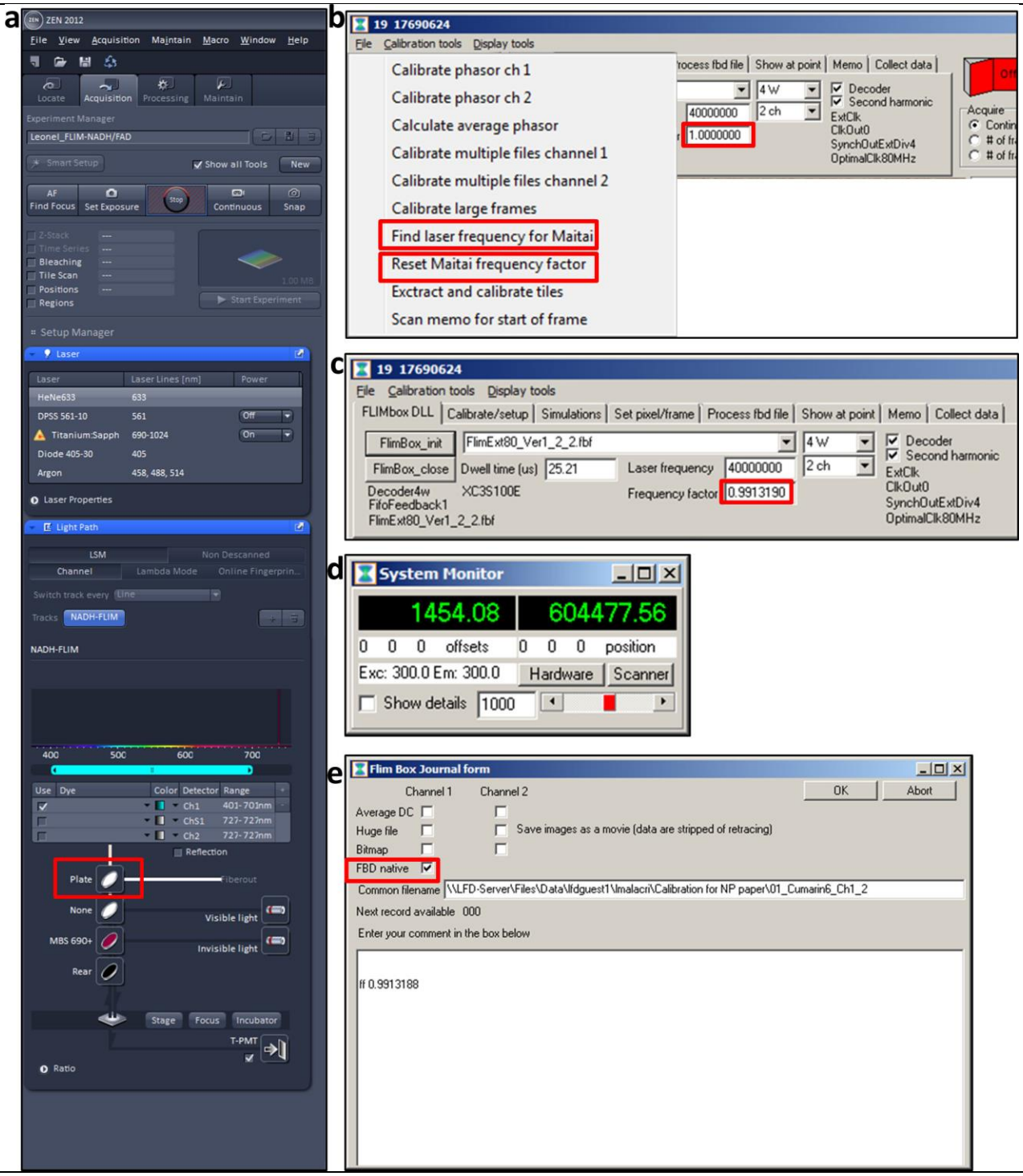

Supplementary Figure 7

Setting up the optical path in a commercial microscope and calculation of frequency factor for proper synchronization of FLIM imaging using FLIMbox.

a) Choosing the right light path and continuous scan using the Zen software. b-c) Calculation of the frequency factor, d) system monitor to monitor counts/s and e) Saving FLIM data from FLIMbox.

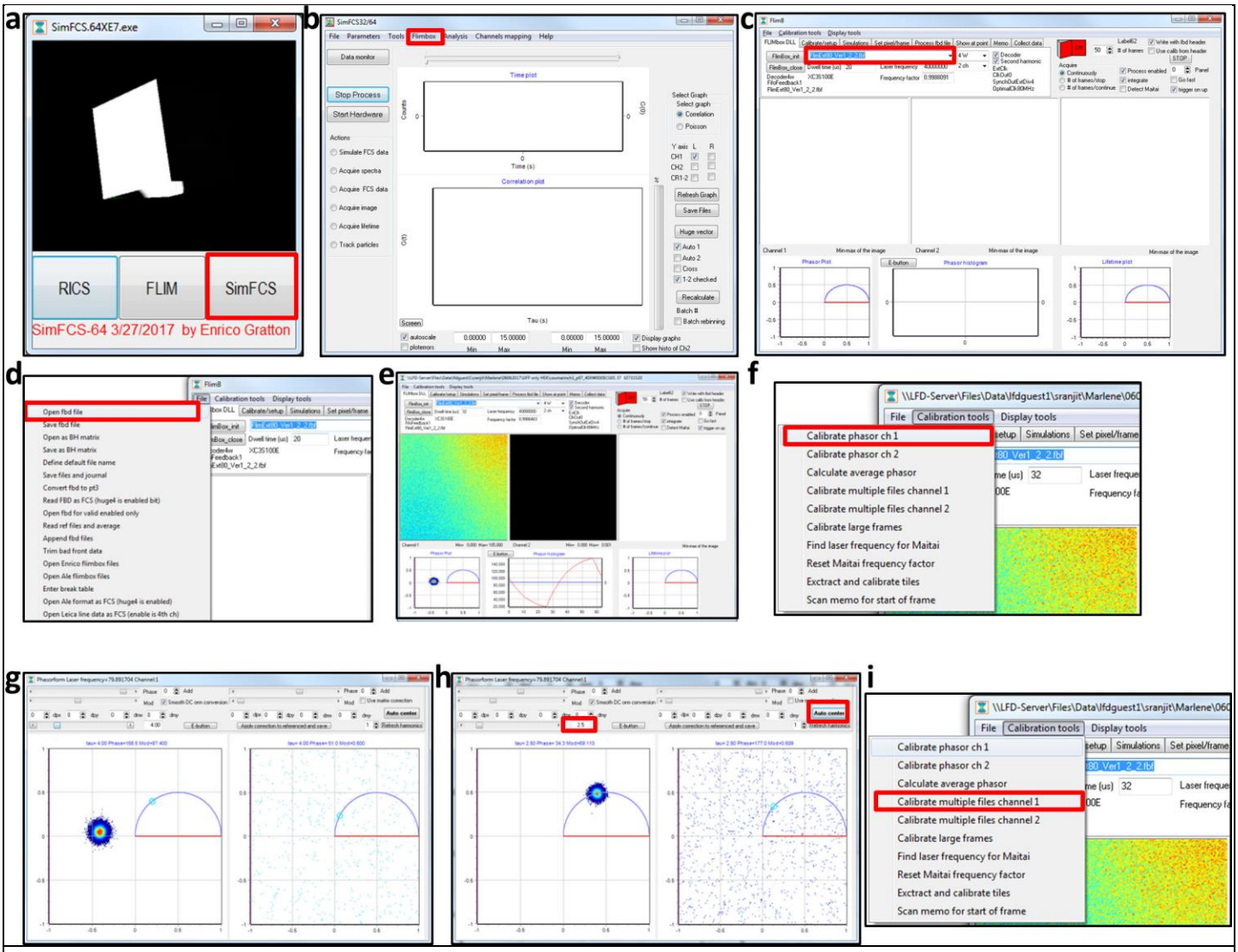

Supplementary Figure 8

Calibration of phasor plots using a known lifetime standard and using the calibration factors to calculate phasor positions of unknown lifetime samples.

a) SimFCS software. b) Acquisition window. c) FLIMbox window. d) Opening the Coumarin 6 .fbd file. e) Corresponding image after opening. f-h) Calibration using the Coumarin6 for Channel 1. i) Calibration of multiple files using the Coumarin 6 as calibration standard.

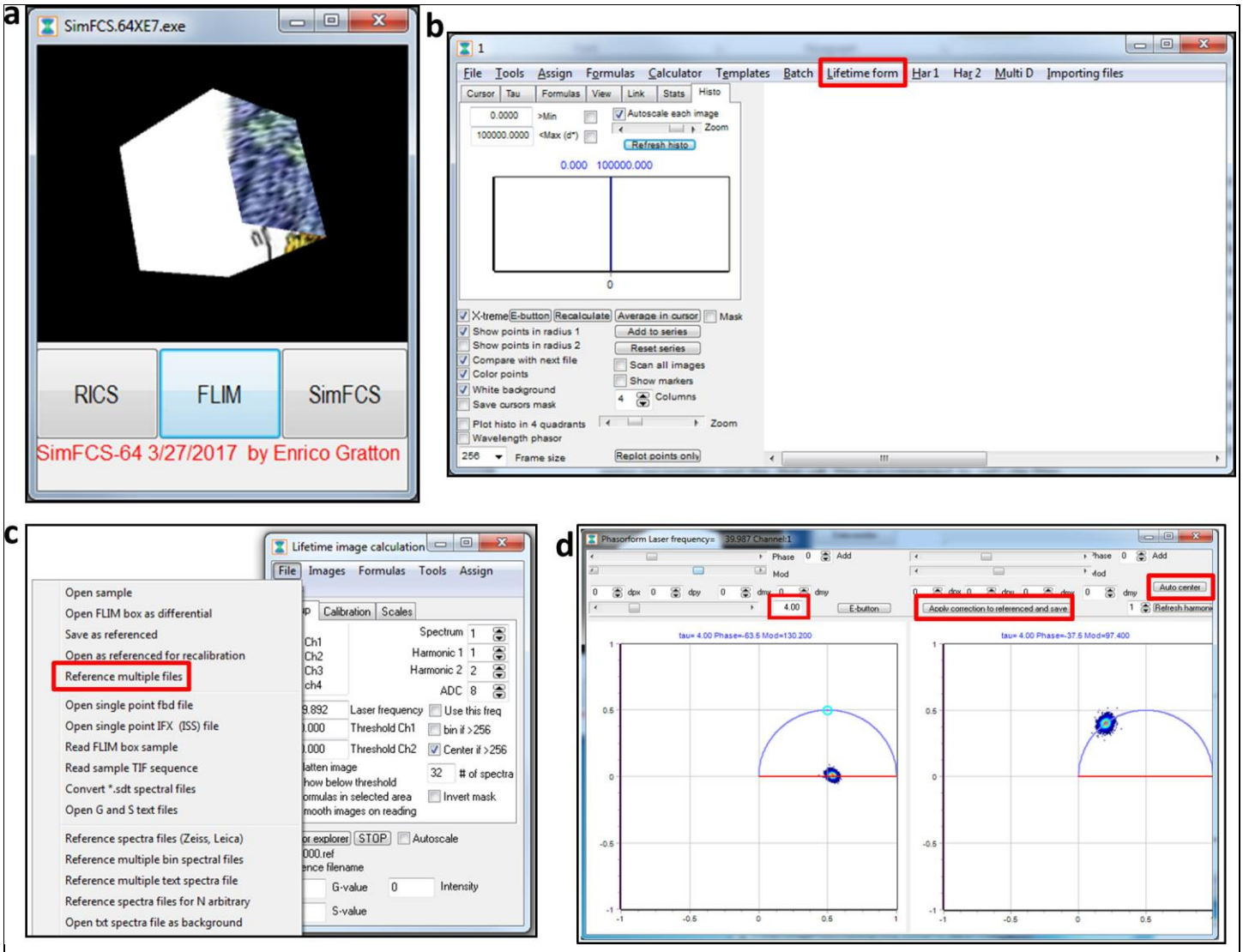

Supplementary Figure 9

Referencing multiple files and conversion to referenced (.ref/ .r64) files.

a) The SimFCS software. b) FLIM analysis window. c) Lifetime image analysis window. d) Phasor calibration using known lifetimes.

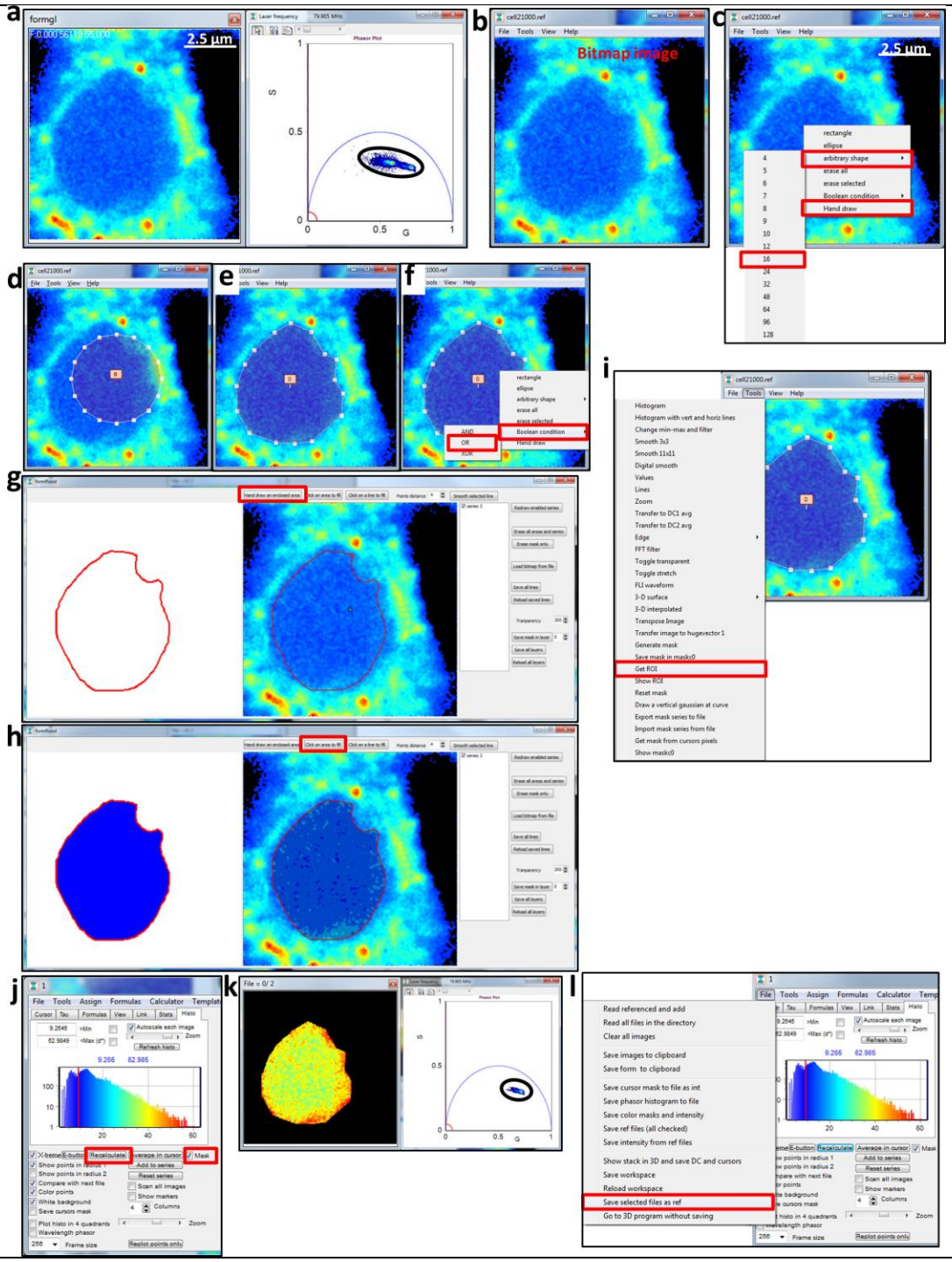

Supplementary Figure 10

Masking FLIM images using SimFCS routine.

a) FLIM image of a cell and corresponding phasor plot. b) Bitmap image, and selection of masking parameters. d-f) masking procedure using a shape. g-h) Hand-drawn masking. i) Selection of ROI. j) Application of the ROI. k) The masked nucleus and the corresponding phasor plot. l) Procedure to saving the masked reference file.

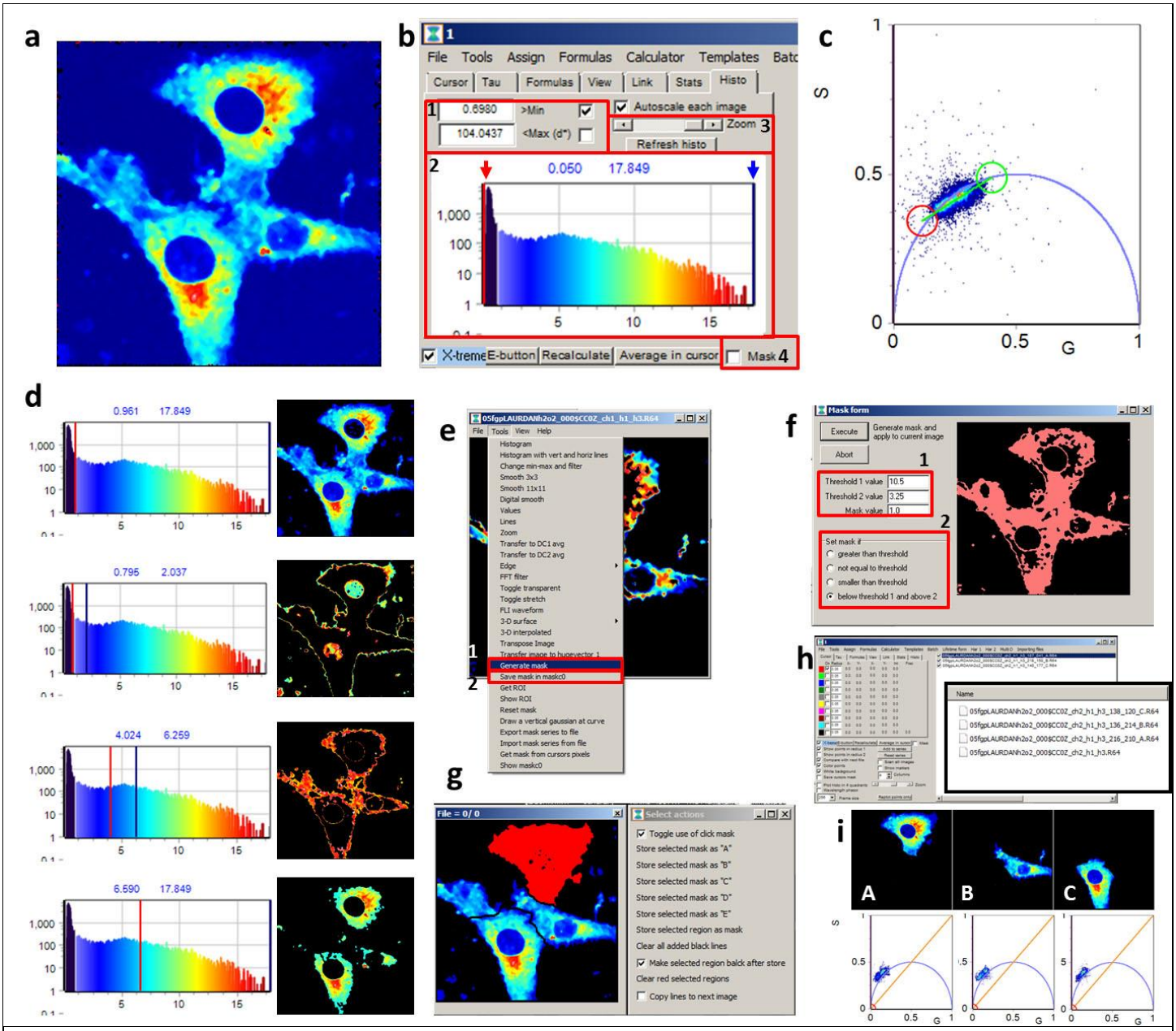

Supplementary Figure 11

Masking by intensity using SimFCS.

a) Select a file for masking. b) Thresholding the histogram to select the region of interest. c) Phasor plot for the first threshold in section d. e and f) Masking using the histogram threshold value. g-i) Rapid masking of different areas in the image.

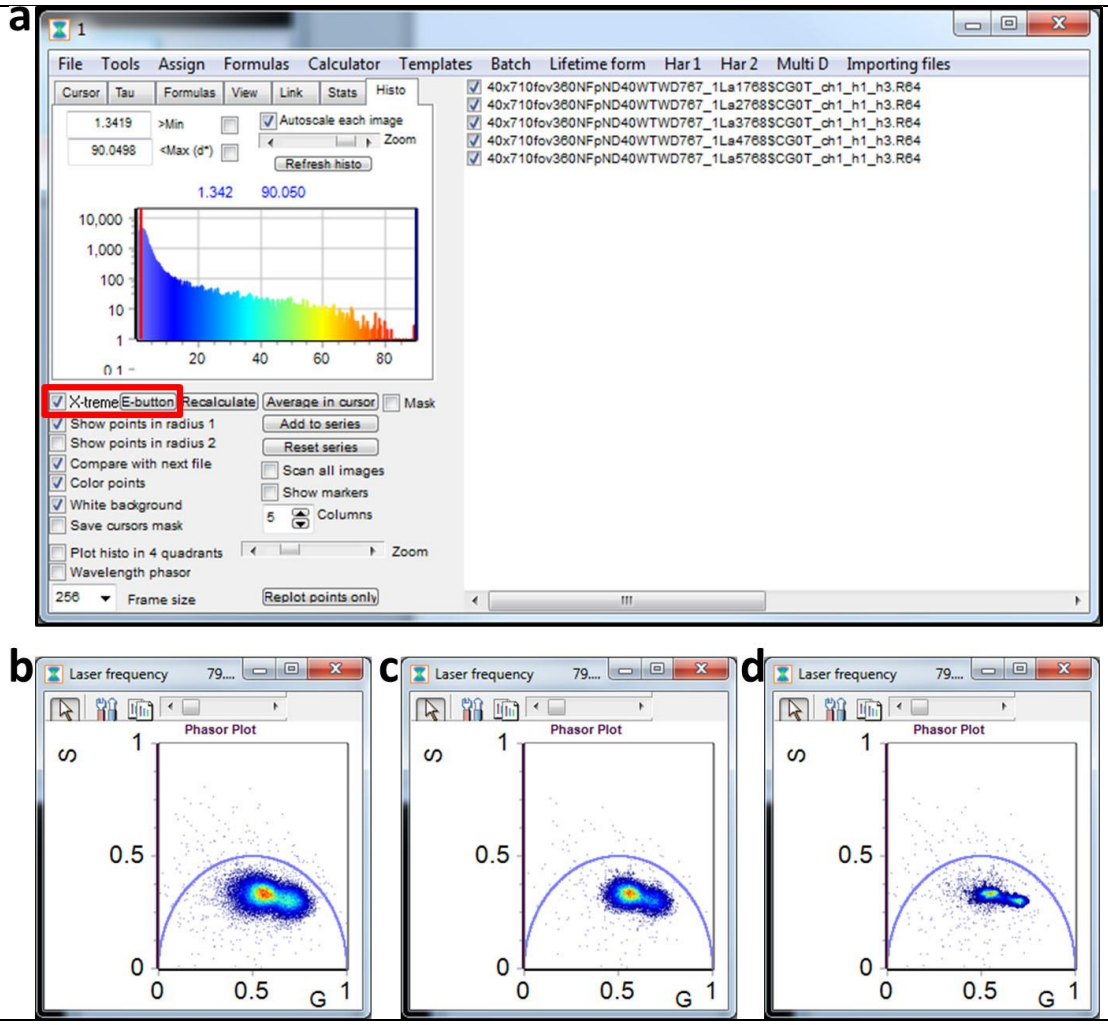

Supplementary Figure 12

Filtering the distribution of phasor points in the phasor plot.

a) The buttons for filtering. b) Phasor distribution after no filtering, c) 3x3 normal filtering, and d) 5x5 ‘X-treme’ filtering.

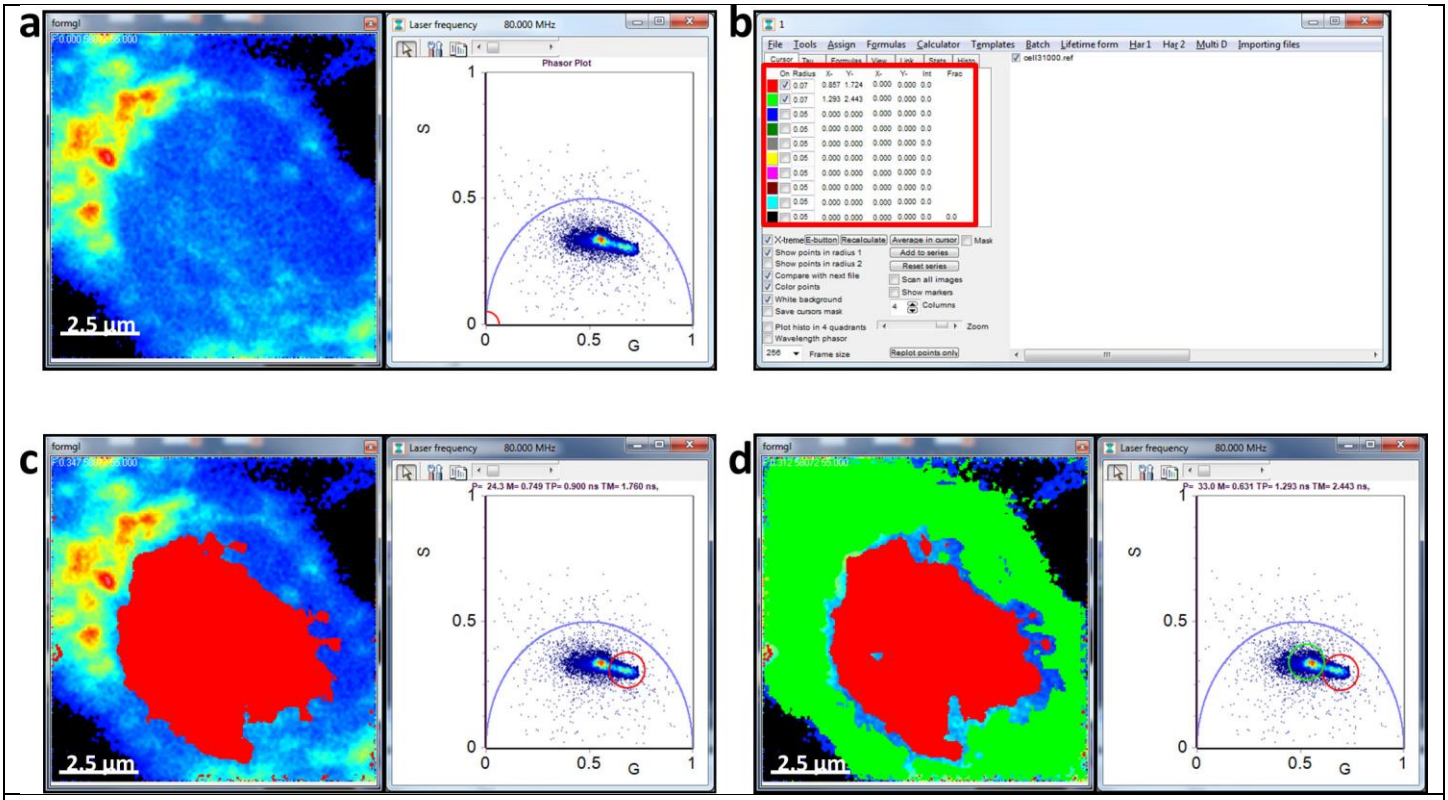

Supplementary Figure 13

Selecting part of a phasor plot and painting the image accordingly.

a) The intensity image of phasor coordinates of a MEF cell. b) Selection of the cursors. c-d) Painting the image according to phasor selection.

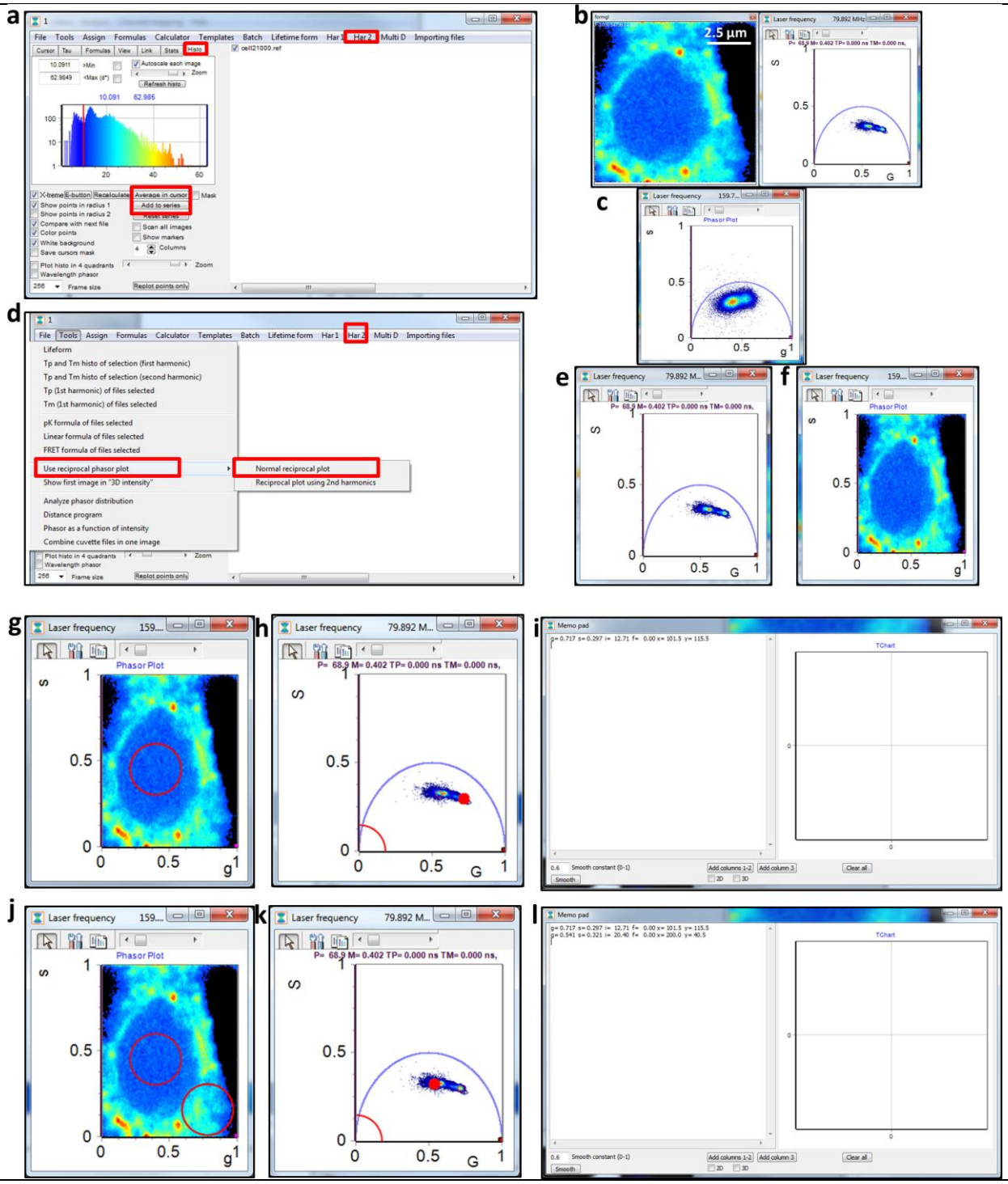

Supplementary Figure 14

Reciprocity principle and finding phasor coordinates originating from a selected area of an image.

a) FLIM analysis window, histogram min-max correction. b) Corresponding FLIM image and phasor histogram. c) Second harmonic window. d) Transferring the image to the second harmonic window. e) Phasor plot. f) The harmonic window. g) Choosing an area of an image. h) Position of the phasor points arising from the chosen cursor and saving the data to the Memopad (i). j-l) Continuation of the analysis in a different part of the image.

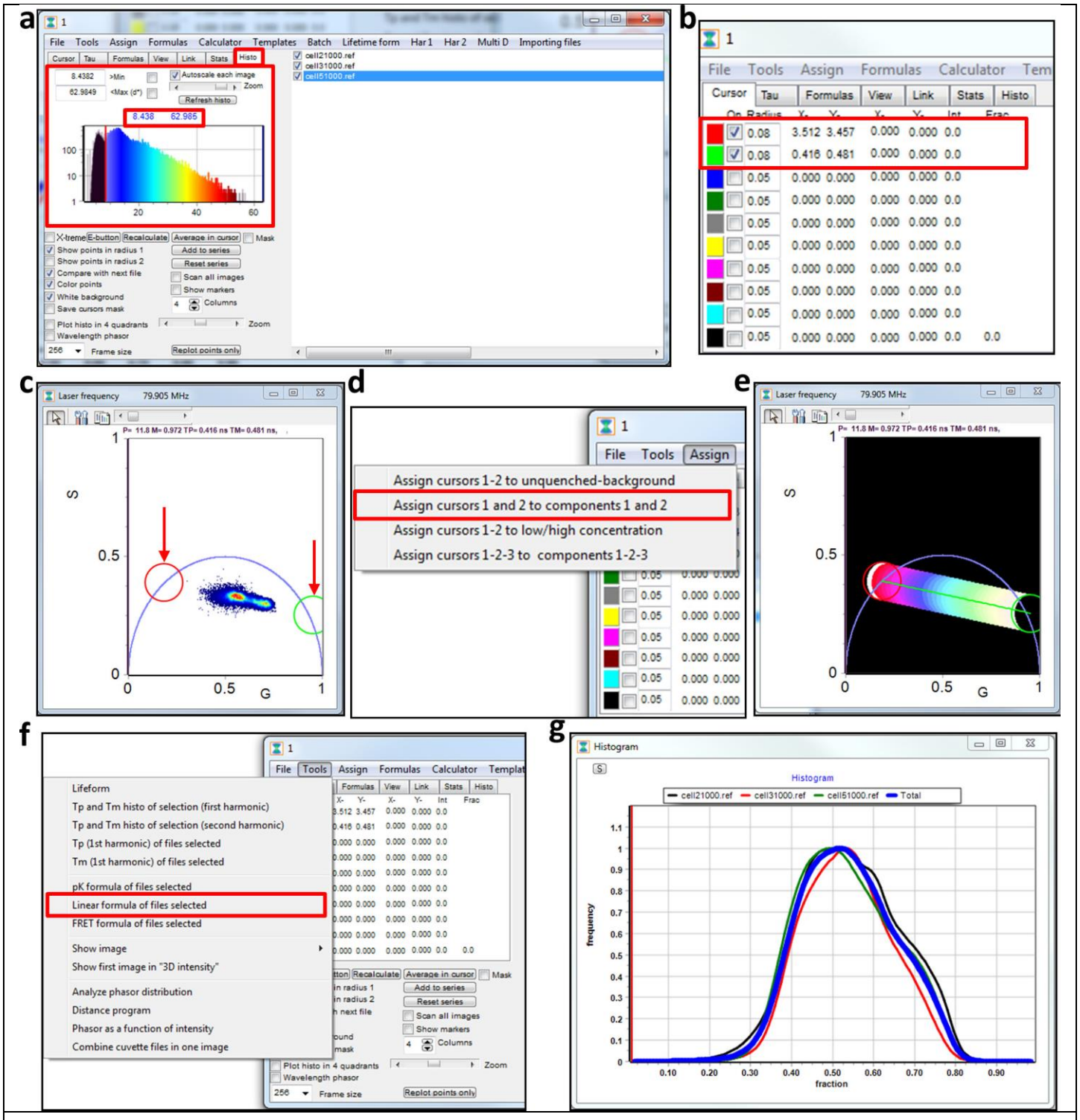

Supplementary Figure 15

Analysis of phasor histogram for two components using linear additive properties of phasor plot.

a) Opening files and selecting min-max using histogram. b) Selection of cursors. c) Positioning the cursors along a metabolic trajectory. d) Assignment of the cursors. e) Linking of the cursor in phasor plot. f) Using linear formula to covert the phasor histogram to the distribution of two species (Supplementary Figure 14g).

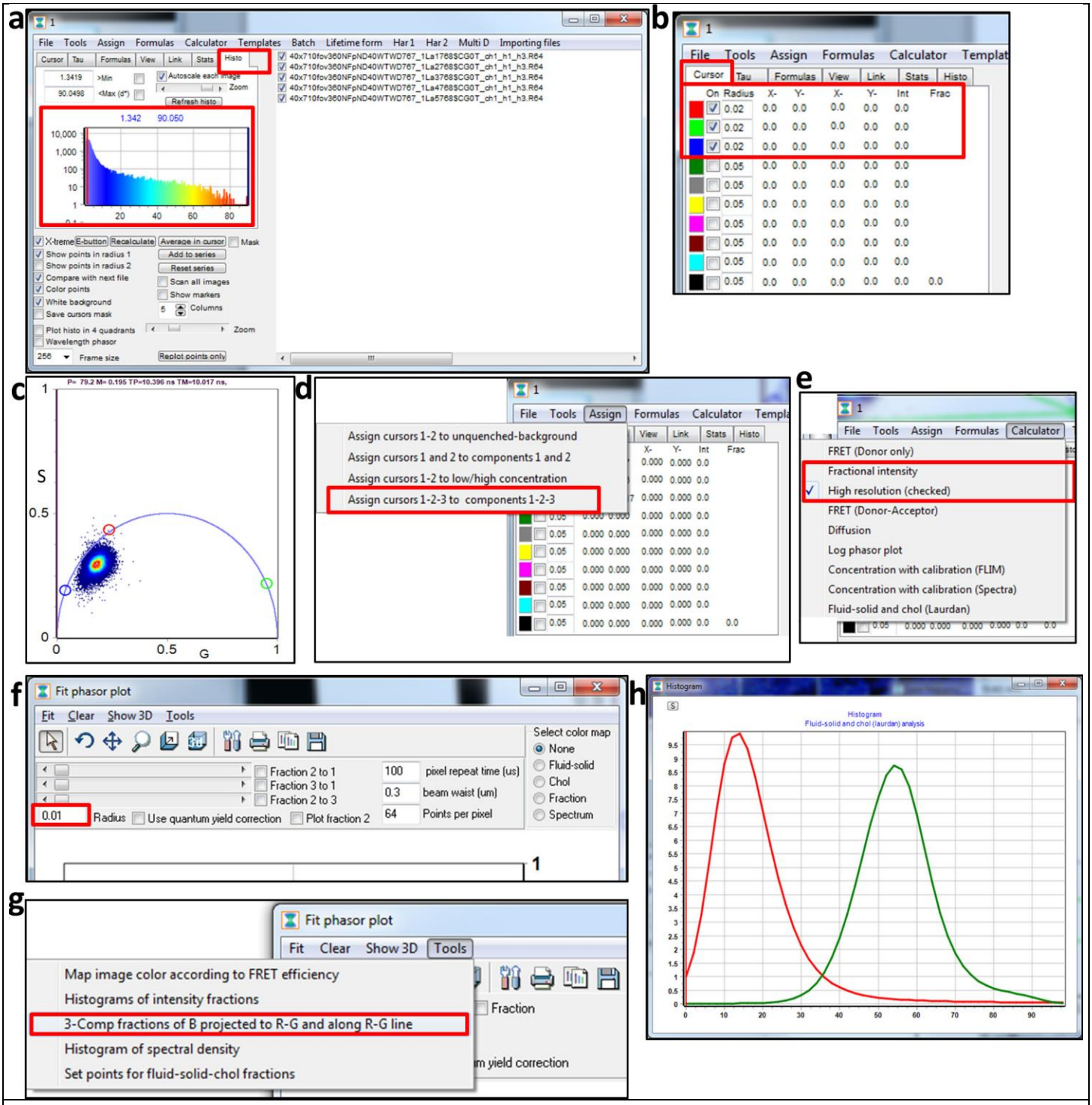

Supplementary Figure 16

Three component analysis using phasor plots.

a) Histogram to check intensity. b) Selection of three cursors for the 3-component analysis. c) The positions the three cursors in the phasor plot. d) Assignment of the three cursors. e) Conversion to the 'Fit phasor plot'. f) 'Fit Phasor plot' window and choosing the radius of the cursor, g-h) Calculation of the fraction along the axis connecting red and green cursor (red plot) and fraction of 3rd component (green plot).

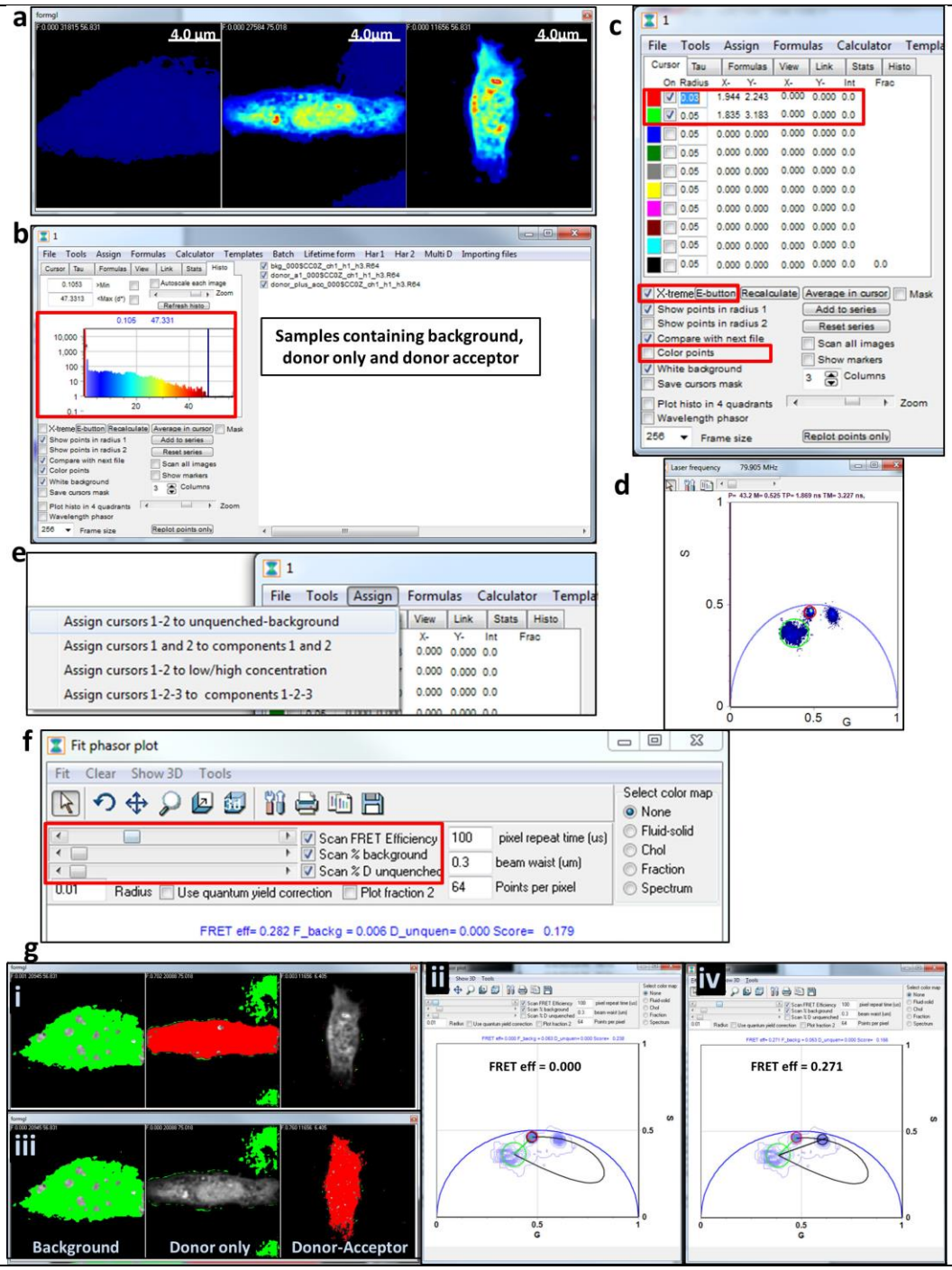

Supplementary Figure 17

Analysis of FRET using phasor approach.

a) Intensity image of autofluorescence background, donor and donor-acceptor samples. b) Analysis window and histogram selection to reduce the background from unmodulated light. c) Selection of cursors, filtering of data, and changing the image to grayscale. d) Phasor positions and selection of background and donor only sample. e) Assignment of the cursors. f) FRET calculation sliders. g) Phasor mapped intensity images for donor only (i) and donor –acceptor (iii) samples and their corresponding FRET trajectory positions (ii and iv). The calculated FRET efficiency is 0.27. The curved lines in the figure are not the result of a fit but just the application of the rule of linear combination of 3 phasors.

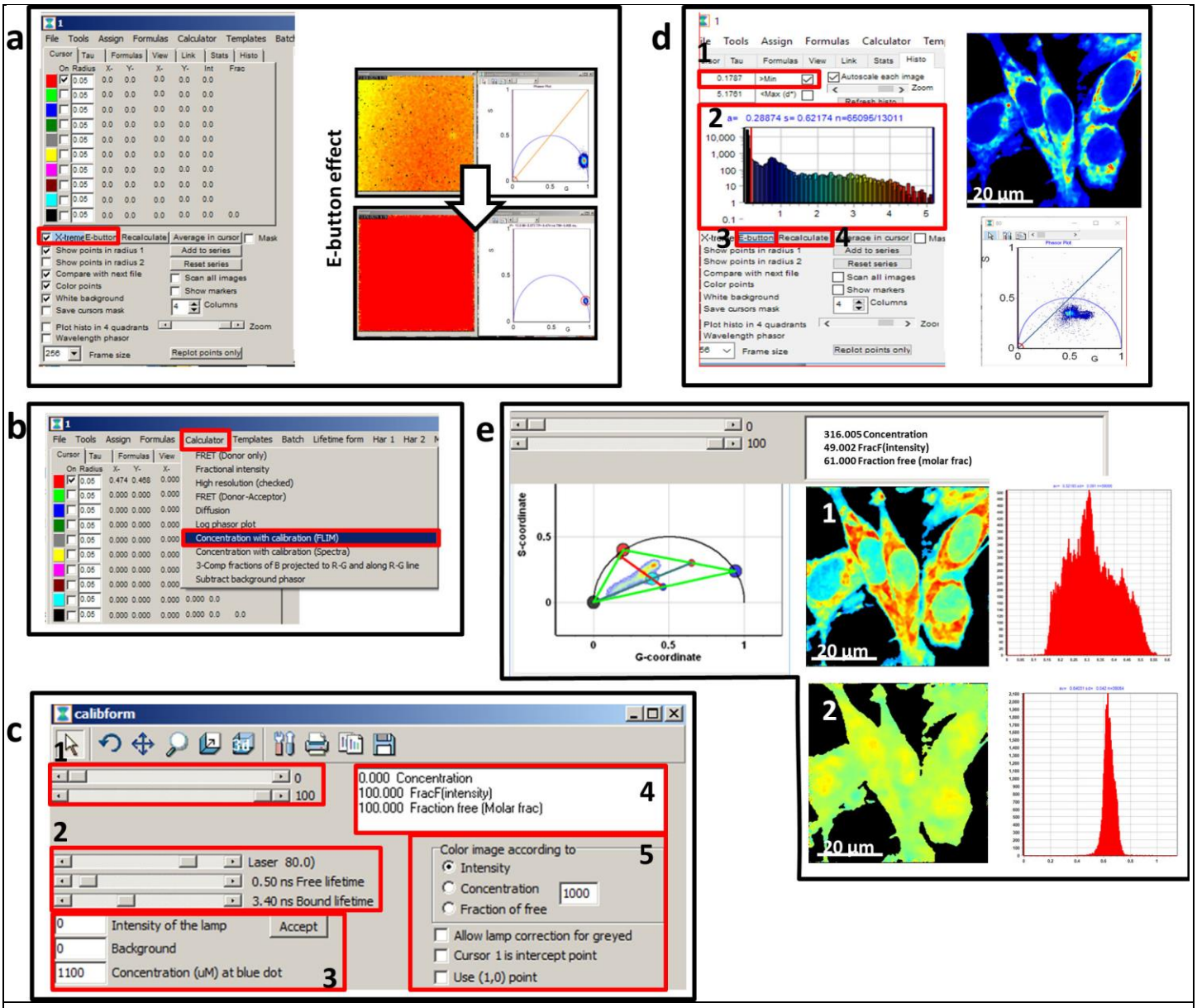

Supplementary Figure 18

Calculation of absolute concentration using phasor approach.

a) Loading and filtering of calibration standard of known concentration of free NADH. b) Accessing the calibration page. c) Options in calibration page. d) Histogram correction and loading of experimental images. e) Calculation of the modified trajectory of phasor point based on addition of unmodulated light and calculation of the different quantities and mapping the image according to concentration of NADH (top) and free to bound NADH ratio (bottom).

SUPPLEMENTARY METHOD

The following section describes the steps required for FLIM data acquisition using a commercial confocal laser scanning microscope (Zeiss LSM 710, in this particular example).

Steps for FLIM data acquisition

FLIM acquisition ● Timing 60-90 min

The following steps describe the acquisition procedure using the FLIMbox mode utilizing a Zeiss LSM 710 confocal microscope with a 40X 1.2 NA water immersion objective. In the FLIMbox mode, the Zeiss 710 sends a 'beginning of frame signal' that is recorded by the FLIMbox and used to assign each photon to the corresponding pixel of the image.

i. First place the sample on top of the objective and image using the 'continuous' scan image option (box 1, Supplemental Figure 6a). Set the scan in the 'frame' mode and choose a frame size of 256x256 (box2, Supplemental Figure 6a). Set the pixel dwell time as 25.21 µs and the line step as 1. Depending on the sample fluorescence, lifetimes using the FLIMbox mode are usually acquired with 16 µs to 32 µs pixel dwell times.
ii. Synchronize the FLIMbox and Zeiss software (Zen) and hence choose no averaging (Supplemental Figure 6a, box 3) and no repeat lines.
iii. Choose the proper pulsed laser wavelength and power using box 4 of Supplemental Figure 6a. The Zeiss LSM 710 has an AOM already installed internally that can control the power of the Ti:Sapphire excitation laser. In the absence of an internal AOM, use an external AOM to control the laser power.
iv. The path of the emitted light is controlled using box 5 of Supplemental Figure 6a. In this box configuration, select the mirror, which results in the fluorescence being detected by the Zeiss detector and thus selects the proper areas for imaging. Change this window to 'plate' to direct the signal towards the outside detector.
v. Open the SimFCS software and press 'SimFCS' to open the acquisition window (Supplemental Figure 6b).
vi. Select the proper input card (FLIMbox) and scanner (Zeiss scanner) by opening the 'Hardware' portion of the 'Parameter' button of box 1, Supplemental Figure 6b. This window (Supplemental Figure 6c) has multiple options for controlling the microscope using SimFCS which are not utilized here. If any of the hardware components are added or deleted in the 'parameter' window called 'defaultsform', then SimFCS needs to be restarted to properly register the hardware configuration.
vii. Open the FLIMbox window by clicking the button for red box 2 of Supplemental Figure 6b. This operation opens the window in Supplemental Figure 6d. Select the proper FBF (FlimBoxFirmware) configuration file for the FLIMbox firmware (needed for the selected laser - 20MHz for supercontinuum laser and 80 MHz for TI-Sa laser)) using the red box in Supplemental Figure 6d.

viii. At this point, store the proper values of the acquisition in the 'FLIMbox' window, so that the appropriate synchronization can be achieved. This synchronization includes the matching pixel dwell time 25.21 µs, frame size of 256x256, line time and frame time. The line time (15126 µs) is much longer than pixel dwell time x 256 as this also includes retracing time of the Zeiss 710) and the line length includes the total pixels of the image + retracing pixels. Also choose the microscope type and proper laser (red box Supplemental Figure 6e).

ix. Once the proper values are set, initialize the FLIMbox using the 'FLIMbox_ini' button (red box Supplemental Figure 6d). This command sends the proper firmware to the FLIMbox. It is needed only if the firmware is changed. This operation results in illumination of the 'Clock Frequency' light at the front of the FLIMbox (Figure 4c).

x. Now reflect the light towards the outside detector using the option 'plate' of the red box in a. Turn on the yellow buttons in Figure 4c for the detector power supply and collect the signal using the external detectors.

xi. First press the red acquisition button of the SimFCS FLIMbox acquisition (Supplemental Figure 6e). The FLIMbox will stay idle until the start of frame signal is detected. Then press the 'continuous' button (Zen) in Supplemental Figure 7a for the acquisition and the FLIMbox will start recording the photons. Two sequential steps are needed for the FLIMbox to record the signals from the Zeiss unit. If the FLIMbox is turned on after the Zeiss 710 starts scanning the first frame will be lost.

xii. The proper frequency factor for the laser is required for frequency domain measurements and calculation of the phasor plot. Multiplying the frequency factor by the laser frequency determines the period. First reset the frequency factor using the 'Reset Maitai Frequency factor' button under 'calibration tools' tab in Supplemental Figure 7b.

xiii. The frequency factor is required because the FLIMbox is synchronized with the laser period, which in general is wavelength dependent, while the scanner frame period depends on the internal clock of the Zeiss microscope. Some of the newer FLIMboxes have an internal frequency counter which detects the laser frequency so that calibration of this frequency is no longer required.

xiv. To find the actual frequency factor, take three scans and then press the 'Find laser frequency for Maitai' button under 'calibration tools' tab (Supplemental Figure 7b). The proper frequency factor is shown (0.9913190 in this case, all figures are significant) (Supplemental Figure 7c). The frequency factor can also be obtained after the measurement by reapplying the acquired sequence.

xv. Monitor the fluorescence intensity using the 'system monitor' window (Supplemental Figure 7d) which directly measures the counts/s as seen by the detectors.

xvi. Now repeat step xi to start acquisition. Once sufficient photons are acquired, first turn off the red acquisition button in FLIMbox page and then press the 'stop' button in LSM710 set up to close acquisition. Either set the number of scans prior to starting acquisition for a known number of repeats or acquire data continuously until a certain number of photons are counted (Supplemental Figure 7d).

xvii. To save the data, open the 'FLIMbox Journal Form' window using the 'file' option in the FLIMbox window (Supplemental Figure S7e) and select 'Save files and journals' button (Supplemental Figure 7e).

xviii. Check the 'FBD native' (FBD= FLIM Box Data file) button in the window of Supplemental Figure 7e and place the file name along with the file in the 'common filename' window. Often the frequency factor and other details are saved by writing them in the open box and then pressing the OK button (Supplemental Figure 7e).

xix. This procedure saves two files. One with extension .FBD which is a FLIMbox data file and includes the time of arrival of each photon in the number of channel selected. The other file is a journal file with a .jrn extension that contains all the details of the experiment including any details typed in the open area of Supplemental Figure 7e.

xx. Once the first FLIM image is acquired, choose a new area by selecting the 'mirror' option in Supplemental Figure 6a and the Zen software. Then alter the light path back to 'plate' (Supplemental Figure 7a) and repeat the acquisition procedure to obtain the FLIM data.

xxi. Finally, measure a lifetime calibration standard using the same excitation wavelength and the FLIM images will be calibrated against these standards.

xxii. The next three steps are specific to the acquisition of absolute concentrations.

xxiii. Use a solution of free NADH (~1 mM) (known concentration) for the absolute concentration calibration (ε_{340nm} = 6220 $M^{-1}cm^{-1}$).

xxiv. Calibrate the lifetime phasor with a solution of a known fluorescence lifetime (Coumarin6 or Rhodamine 110) and fix the following parameters - laser power, excitation wavelength (740 nm for NADH), pixel dwell time (between 10-30 µs/pixel) and number of frames (usually between 30-40 frames) to acquire the lifetime from the samples. Acquire the NADH calibration solution at the end using the same parameters used for the other images.

SUPPLEMENTARY NOTE 1

Metabolism measurements based on FLIM

Autofluorescence from cells has traditionally been used as an index of metabolic activity in cellular systems[23,24]. Two cofactors, NADH and FAD, are universal in any life form and they participate in cellular metabolic activity. Some oxidation states of these two cofactors are fluorescent. The equilibrium between NADH and NAD+ and the redox oxidation states of FAD are indicative of the metabolic state of cells[25-27]. NAD+ is non-fluorescent and does not contribute to autofluorescence. Hence, traditionally, intensity ratios related to NADH/FAD or NADH/(NADH+FAD) have been used for understanding metabolism using fluorescence measurements[26,28]. This approach is experimentally possible due to the difference between the excitation and emission spectra of NADH and FAD and the possibility of using two-photon excitation in tissues to minimize scattering and tissue damage. In two-photon excitation, both NADH and FAD can be simultaneously excited and then bandpass filters can be used to isolate their respective emissions. However, intensity based ratiometric measurements always have an underlying assumption, namely, that only two individual species (in this case NADH and FAD) contribute to the emission and that the quantum yields of the two fluorophores are independent of their physical states and environment. This assumption is actually invalid when considering NADH and FAD. Free NADH has a fluorescence lifetime of 0.4 ns and a very low quantum yield[41]. The lifetime of NADH increases considerably when bound to a protein, e. g. binding to lactate dehydrogenase (LDH) in the presence of oxalate increases the lifetime to 3.4 ns[6]. FAD shows a reverse trend[29]. Specifically, FAD is fluorescent and the reduced form $FADH_2$ does not show significant fluorescence. Furthermore, when bound to proteins the quantum yield of FAD decreases significantly and a similar trend is observed in its fluorescence lifetime. Fluorescence contributions from NADH and FAD can be complex and the ratiometric measurements commonly employed may oversimplify the issue. However, it has been shown that the ratio of NAD+ to NADH is related to the ratio of free to bound NADH and that this ratio can be used to monitor changes in metabolism[26]. A change towards increased free NADH is representative of more glycolytic metabolism and less oxidative phosphorylation (Figure 8a-d)[26,30]. A change in this ratio can be indicative of the metabolic state of the cell. This ratio can be quantified by determination of the position of the phasor points from autofluorescence obtained through a narrow blue filter (440-490 nm bandpass) which selects primarily NADH emission. The free NADH lifetime (0.4ns) is very close to the s=0, g=1 position of the phasor plot (at 80MHz; blue cursor, Figure 8e). The position of bound NADH (e.g. to LDH) is close to s=0.3, g=0.2 (cursor green, Figure 8e) in the phasor plot (at 80 MHz). In the absence of other fluorescent species, the autofluorescence arising from NADH corresponding to different fractions of free/bound NADH is spread along the line joining these two points in the phasor plot. This line is called the metabolic trajectory and a shift along this trajectory can be exploited to study changes in metabolism (Figure 8e)[10]. This change of the phasor position along the trajectory has been traditionally analyzed using the following two approaches.

The first type of analysis involves changes in the average phasor position[1]. This approach relies on determination of the average phasor positions from each of the images followed by comparison of these average positions between sets of images. This type of analysis is explained in section 5B on analysis of FLIM samples. The other type of analysis is based on representation of the position along the

metabolic trajectory with colors. This approach is based on the linear addition properties of phasor space. According to the law of phasor addition, the position of a phasor point arising from contributions from two different original points is on the line joining those two original points[11,31]. The contributions of these two original points to the position of this phasor point are inversely proportional to the distance of the new phasor point to each of the original points[21,31]. The heat map derived from the line of linear combination in a phasor plot is used to color an image according to the position of a pixel (of the image) along the line of the metabolic trajectory (in the phasor plot). In the presence of a third component (an as yet unidentified long lifetime species (LLS) ~ 7.8 ns, believed to be due to oxidized lipids[10]), the autofluorescence signature changes significantly and thus requires a different type of analysis to convert the phasor heat map to the fraction of free NADH. This 3-component analysis is based on the same linear addition phasor properties used for the two component analysis. The details of the analysis are explained elsewhere[11]. According to the phasor addition properties, if the experimental phasor point originates from three individual phasor points, then this point must lie inside the triangle joining those three individual phasor points. A line passing through the third point and the experimental phasor point intersects the metabolic trajectory (Figure 8e). This point of intersection is used to calculate the ratio of bound to free NADH (Figure 8e) using the following equation

$$Fraction\ of\ free\ NADH = \frac{distance\ (intercept\ to\ bound)}{distance\ (free\ to\ bound)}$$

The fraction of the third component (Figure 8e) can be calculated based on the equation,

$$Fraction\ of\ third = \frac{distance\ (experimental\ point\ to\ intersect)}{distance\ (intersect\ to\ third\ component)}$$

Using this procedure, the phasor distribution can be converted to the metabolic distribution when a third individual component is present. These two methods of analysis let us extract the lifetime information in the NADH channel corrected for the contributions of other species that otherwise could be incorrectly assigned to metabolic aspects.

SUPPLEMENTARY NOTE 2

Förster resonance energy transfer (FRET) and phasor plots

FRET is a physical process involving transfer of excited state energy from a fluorescent molecule (donor) to another molecule (acceptor), which results in a decrease in the lifetime of the donor fluorophore[32]. Figure 9 shows the change of phasor position due to FRET in the absence and presence of a contribution due to fluorescence background. This figure shows that in the presence of FRET, the phasor of the donor follows a specific trajectory that can be easily identified and attributed to FRET.

FRET based biosensors have been used to assess a variety of intracellular processes including kinase, phosphatase, and GTPase activities, messenger RNA dynamics, receptor interactions and more recently to assess metabolism[3,33,34]. These biosensors are usually synthesized using two separate strategies, i.e., the dual chain and the single chain approach (Figure 10a)[3]. In the dual chain approach, two individual proteins are tagged with fluorescent moieties, i.e., FRET pairs. In this system, in the absence of any interaction, the donor's fluorescence is not altered. But if the two proteins interact, the distance between the FRET pairs is reduced and the donor transfers energy to the acceptor resulting in a decrease in the donor lifetime. The single chain approach involves having both the donor and acceptor connected to the same protein complex. In this case, even in the absence of the target ligand, the FRET pair may be close enough to experience some extent of energy transfer. But once there is a change in the structure of this complex, due to ligand binding, the distance between the donor and acceptor can alter significantly, resulting in a change in FRET efficiency (Figure 10b).

The changes in lifetime due to FRET can easily be analyzed by the phasor approach[37]. The FRET trajectory for the donor is curved as the donor lifetime is gradually quenched by the FRET process. The extent and shape of the FRET trajectory inside a phasor plot is dependent on the contribution from any autofluorescence. However, biosensors have two states differing in FRET and hence donor lifetimes, rather than displaying a gradual change in FRET efficiency. The two states have their own corresponding phasor positions. Thus FRET biosensors are inherently similar to the two species system. The position of the measured phasor position lies on the straight line joining the phasor positions of the low FRET and high FRET states. Following the linear combination properties of phasors the fraction of molecules undergoing FRET can be calculated from the distance of the experimental phasor point to the phasor positions of the high and low FRET states. The autofluorescence of cells can contribute in biosensor FRET measurements and thus autofluorescence under the same excitation wavelength is required for the calculation of the trajectory[3]. An example of FRET biosensor is shown in Figure 10c. The top panel of Figure 10c shows the intensity images of RhoA-biosensor upon LPA (lysophosphatidic acid) activation. The intensity images are similar to each other. Bottom panel of Figure 10c shows the phasor mapped FLIM images of the same cell. LPA enables binding of RhoA with rhotekin fragments resulting in change of FRET efficiency of the biosensor. Changes of the FRET efficiency with time can be observed from the FRET trajectories in the phasor plots shown in the middle panel of Figure 10c.

SUPPLEMENTARY NOTE 3

Calculation of absolute concentrations (free and bound NADH).

Measurement of the absolute concentration of a metabolite inside a living cell is very challenging from a classical biochemistry point of view. In the case of NADH, the fluorescence lifetime and quantum yield may change upon binding to specific enzymes [38, 39] and these changes can be exploited to measure the ratio of free to bound NADH in a live cell. As discussed earlier, these ratios can then be correlated to metabolic states[1,,30,40,]. However, these changes in quantum yields complicate the measurement of the absolute concentration of NADH in a cell using a simple external calibration such as measuring the fluorescence from a solution of known concentration**.** To avoid this problem, a method to determine the absolute concentration of NADH in cells with high pixel and temporal resolution (60 s), based on phasor plots has been developed. This method is based on the introduction of unmodulated light which will interfere with the measured lifetime of the free/bound NADH[6]. The expected position for unmodulated light in the phasor plot is at the (0, 0) coordinate. In the presence of this unmodulated light, the distribution for the free/bound NADH will be shifted toward (0, 0) and the extent of this shift is determined by the amount of unmodulated light and the fluorescence intensity at each pixel. This relative movement based on the pixel intensity results in the calculation of absolute concentration of free and bound NADH using a calibration standard of free NADH. It is important to clarify that "real" external unmodulated light is not necessary and that "virtual" unmodulated light can be added using SimFCS software and that this calibration is linear over the range of the experiments. The mathematics for the calibration is based on the rules of phasor addition. Mixing a component with a particular lifetime (0.4 ns for free NADH) with a second component with an infinite lifetime (unmodulated light) results in a distance (M) from the origin for the s and g coordinates given by:

$$M = \frac{L}{L + F}$$

Where, M, L and F represent modulation, amount of light added and fluorescence, respectively. F can be calculated since M is experimentally determined and L is a known quantity. This calculation is carried out using the projection of M on the x-axis (g-coordinate):

$$g = g_0 \frac{L}{L + M}$$

g_0 represents the g-coordinate before external light addition, then L and M are known quantities.

Figure 11a shows the shift of the calibration solution based on the extent of unmodulated external light. The blue and black circles show the center position for the free NADH calibrator solution and the unmodulated light, respectively. Increasing the amount of unmodulated light shifts the final position of the NADH calibrator solution toward the (0, 0) position. Figure 11b shows the experimental phasor points for free and bound NADH. The cursors can be moved to define the position of free (blue) and bound (red) NADH. The green triangle encloses the area for all possible linear combinations expected for the three component system, unmodulated light being the third component. The calibration is processed by adding some unmodulated light to the phasor plot and then moving the red line to the

resulting phasor positions of free and bound NADH. This operation defines the concentration of the solution (Figure 11c) for the resultant phasor positions. The shift in the position of free NADH is larger than the one for the bound NADH. The quantum yield for the bound NADH is approx. 8.5 times larger than for the free NADH (estimated by the difference in lifetime[41]), and final shifts in the coordinates are calibrated taking this difference into account. Finally the red line in Figure 11b represents a concentration of NADH independent of the fraction of free and bound. The range of concentrations measured is limited to the highest concentration of the prepared solution down to zero (red line to grey cursor). Finally, the fraction of free to bound NADH can be estimated by exploring the shift between these two cursors (dashed pink line Figure 11c).

SUPPLEMENTARY NOTE 4

pH determinations

The phasor approach to FLIM was used for pH determinations, using a fluorophore with a lifetime that alters with changes in pH[4]. The example of intercellular pH measurement given here uses a modified form of GFP (E^2GFP)[4] to monitor pH. The fluorescence of this probe can be distinguished from autofluorescence and modulation of phasor coordinates with changes in pH can result into calibration and measurement of the pH of an unknown system. E^2GFP has single protonation equilibrium with a pKa value of 6.78. Changes in the fluorescence properties of E^2GFP with pH are significant. At low pH the emission maxima is at 510 nm, the value of the quantum yield (φ) is 0.10 and a tri-exponential is required to fit the fluorescence decay with lifetime values of 3.49 ns, 1.13 ns and 0.49 ns. At high pH, these fluorescence properties change with the fluorescence maxima shifting to 528 nm, quantum yield (φ) becoming 0.88 and a mono-exponential lifetime of 3.49 ns. First, a calibration of the change in phasor position related to the change in pH is noted and then FLIM images are compared to the calibration curve. This process results in calculation of the pH in the cell and subcellular boundaries. The behavior of E^2GFP is shown in Figure 12a. Two phasor plots corresponding to the modulation frequencies of 40 MHz (left) and 80 MHz (right) are also shown.

The effect of transformation of the changes in pH and the corresponding phasor plot is explained in the following section. This transformation is based on the assumption of a two state model, applicable to the behavior of many pH and other ion indicators. The fluorescence intensity decay from each of these states can be fitted to a multi-exponential decay model, but it has a unique location in the phasor plot. Thus, at any point of the equilibrium the total fluorescence decay, $I_{i,j}(t)$ at a particular pixel coordinate (*i,j*) is given by,

$$I_{i,j}(t) = C_1\left[\sum_k \alpha_k \cdot \exp\left(-{}^{t}/_{\tau_k}\right)\right]_1 + C_2\left[\sum_k \alpha_r \cdot \exp\left(-{}^{t}/_{\tau_r}\right)\right]_2$$

Where, C_1, C_2 are the concentrations of state 1 and 2, respectively, *k* and *r* indices are the exponential components of states 1 and 2, respectively, and α and τ are the amplitude and lifetime.

Once the phasor transformation is applied the resultant phasor position is given by,

$$g_{i,j}(t) = x_1\left[\sum_k \frac{f_k}{1+(\omega\tau_k)}\right]_1 + x_2\left[\sum_r \frac{f_r}{1+(\omega\tau_r)}\right]_2$$

$$s_{i,j}(t) = x_1\left[\sum_k \frac{f_k \cdot \omega \cdot \tau_k}{1+(\omega\tau_k)}\right]_1 + x_2\left[\sum_r \frac{f_r \cdot \omega \cdot \tau_r}{1+(\omega\tau_r)}\right]_2$$

Where, x_1 and x_2 are the molar fractions of state 1 and 2, respectively and $f_n = \frac{\alpha_n \cdot \tau_n}{\sum \alpha_n \cdot \tau_n}$

Thus, these phasor coordinates can be rewritten as,

$$g_{i,j}(\omega) = x_1 \cdot g_{i,j}(\omega)_1 + x_2 \cdot g_{i,j}(\omega)_2$$

$$s_{i,j}(\omega) = x_1 \cdot s_{i,j}(\omega)_1 + x_2 \cdot s_{i,j}(\omega)_2$$

If state 1 and 2 correspond to protonated and deprotonated chromophore, then the molar fractions are connected to pH by the Henderson-Hasselbach equation,

$$\frac{x_2}{x_1} = 10^{(pH-pK_a)}$$

In a two species system $x_2=1-x_1$, and the phasor coordinates can be calculated from:

$$g_{i,j}(\omega) = \frac{g_{i,j}(\omega)_1 + g_{i,j}(\omega)_2 \cdot 10^{(pH-pK_a)}}{1 + 10^{(pH-pK_a)}}$$

$$s_{i,j}(\omega) = \frac{s_{i,j}(\omega)_1 + s_{i,j}(\omega)_2 \cdot 10^{(pH-pK_a)}}{1 + 10^{(pH-pK_a)}}$$

Consequently, the pH of a solution can be calculated, given the phasor positions of the two states and if the pK_a is known, without the necessity of resolving the decay into exponential components. The concept in the pH calculation is first calculation of the molar fraction x_2 which is related to the combination of two phasors. Once the mole fraction is known, pH can be readily calibrated (Figure 12a bottom panel). The Phasor approach allows calculation of the mole fraction directly using the law of phasor addition. The pH calculation is based on the application of the Henderson Hasselbach equation to the molar fractions.

SUPPLEMENTARY NOTE 5

Ion concentration.

The Phasor approach was also exploited to measure epidermal Ca^{2+} gradient using Calcium Green 5N (CG5N)[5]. In this method, phasor points belonging to the highest (p_r) and lowest (p_b) calcium levels are calculated. Then the fraction of the dye bound to calcium (F_b) is calculated after correcting for the relative quantum yield of the calcium free and calcium bound probe. From this fraction (F_b), the calcium concentration can be calculated by using the K_d of calcium green in buffer solution. This calculation is based on the Ca^{2+} ion equilibrium when binding to calcium green. A simple calculation converts the concentration of the Ca^{2+} ion to the F_b. The value of F_b, although obtained as a ratio, arises from the decomposition of the pixel distribution.

The lifetimes of CG5N bound to Ca^{2+} and in free form are different and are easily identified using the phasor approach. The linear distribution of different known concentrations of Ca^{2+} bound to CG5N in-between these two phasor positions show that there are only two species present in this distribution for CG5N and that every point in-between is a linear combination of these two species according to the law of linear addition of phasors (Figure 12b). Once the positions of free CG5N and bound CG5N are calculated, an experimental phasor position resulting from Ca^{2+} binding to CG5N lies on the line combining those two free and bound state points. Thus the position p is given by,

$$\vec{p} = \frac{[Ca^{2+}CG5N]\varepsilon_b\vec{p}_b + [CG5N]\varepsilon_f\vec{p}_f}{[Ca^{2+}CG5N]\varepsilon_b + [CG5N]\varepsilon_f}$$

Where, p_b and p_f are the relative phasor position of bound and free CG5N, respectively, and ε_b, ε_f, and [Ca2+CG5N] and [CG5N] are the relative brightness, and their relative concentrations.

Conversion of this equation gives us the ratio of bound to free dye,

$$\frac{[Ca^{2+}CG5N]}{[CG5N]} = \frac{\varepsilon_f}{\varepsilon_b} \cdot \frac{\|\overrightarrow{p_f - \vec{p}}\|}{\|\overrightarrow{\vec{p} - p_b}\|}$$

This ratio of bound and free dye can be converted to the Ca^{2+} concentration based on the assumption that at equilibrium,

Ca^{2+}.CG5N ⇌ CG5N + Ca^{2+}

And the equilibrium constant is given by,

$$K_D = \frac{[CG5N] \cdot [Ca^{2+}]}{[Ca^{2+}CG5N]}$$

Now, the fraction of dye bound is

$$F_B = \frac{[Ca^{2+}CG5N]}{[CG5N] + [Ca^{2+}CG5N]} = \frac{[Ca^{2+}CG5N]/[CG5N]}{1 + [Ca^{2+}CG5N]/[CG5N]}$$

Combining these equations results in the calculation of concentration of Ca^{2+} ion, where,

$$[Ca^{2+}] = K_D \cdot \frac{F_B}{1 + F_B}$$

The value of K_D can be calculated using a buffer solution and thus the phasor scale can be converted to a concentration scale. The Phasor properties result in the calculation of fractions weighted by the quantum yield. Thus it can be easily transferred to Fb, which, based on a model, can be related to the calcium ion concentration (Figure 12b, bottom panel). SimFCS uses one of these models (which can be specified) and converts the phasor information to F_b and finally to the Ca^{2+} ion concentration. We should note that Hirshfield et al[42] used a phasor approach (although they did not use the term 'phasor') to study calcium binding to Quin2 in cuvette based measurements.

One important aspect of determinations of pH/ion concentration is that the end points of the fluorescence measurements are often required for quantification. Phasor analysis is ideal for such determinations since phasor positions can be easily determined for the beginning and end points in the phasor plot. In solutions, such determinations are very easily realized on unknown solutions. The situations in cells are often much different. The behavior of the probe can be different in cells compared to solutions. Traditionally, efforts have been directed to mimic the cellular conditions to obtain a calibration curve[43–46]**.** This task is very difficult and proper conditions inside the cell can never be exactly replicated. In comparison, the linear addition properties of phasors results in the measurement of the phasors from the two species without physically replicating the cell environment. The linear dependence means that the experimental data points can be extrapolated to find the phasors of the two (bound and free) conditions, these conditions may not be possible to replicate outside the cell. This extrapolation approach gives phasor analysis significant advantages over other FLIM measurements. Once the end positions are known/extrapolated, phasor measurements result in calculation of the molar fraction weighted by the quantum yield of the two contributors. This fraction can be directly related to K_D or pH and those corresponding conditions can be evaluated. In Figure 12b, top right, the phasor position changes with Ca^{2+} binding to CG5N. However, the trajectories are different in cells (black) compared to solutions (purple). Thus, the initial conditions, which are very difficult to obtain, can be calculated based on the phasor approach.

SUPPLEMENTARY NOTE 6

Description of SimFCS software: FLIM module

Fluorescence lifetime images acquired for FLIM signatures can be analyzed using the phasor approach using the SimFCS software developed by Dr. Enrico Gratton at the Laboratory for Fluorescence Dynamics, University of California, Irvine. The software is available from the LFD web site www.lfd.uci.edu. All algorithms used are also available from the same web site. The module for the FLIM analysis in the SimFCS program has been available since 2003, but has been updated and improved over the years and is still under development to include new types of analyses. The details of the phasor approach have been described in earlier sections of this paper. This part is dedicated to an introduction to the FLIM module of SimFCS and various operations available for analysis of FLIM data using SimFCS software. The following paragraphs describe the layout and options of the software interface.

After installing and starting SimFCS, the FLIM analysis module can be accessed through the button highlighted by the red square in Supplemental Figure 1a. Once the FLIM button is pressed, the following two analysis windows open (Supplemental Figure 1b and Supplemental Figure 1c). Supplemental Figure 1b shows the phasor analysis window where the cumulative phasor distribution resulting from the open files is shown and analyses of the image based on the cursor positions are carried out. The blue semicircle represents the “universal semicircle”. Mono-exponential decays results in phasor points located on this semicircle. Multi-exponential decays result in phasor positions inside the blue semicircle (note that certain excited state reactions, such as dipolar relaxation and FRET acceptor emission, can result in phasor points outside of the universal semicircle). Phasor coordinates of g=1, s=0 represent a lifetime of zero and coordinates of g=0, s=0 represent a lifetime of infinity. The average phase lifetime (τ_P) increases with increasing angular position from the G axis. c shows the computer screen that is used for opening and closing files and further data analysis. This procedure is described in detail in the following sections.

The analysis window of the FLIM module is divided into four main subsections - shown in red boxes and designated (i) through (iv) Supplemental Figure 2a to Supplemental Figure 2g. The red box of Supplemental Figure 2 aiii shows image filtering. In this box the E button does a 3x3 pixel median filter of the image. If the X-treme button is checked, the median filter is done on 5x5 pixels. The median filter is only applied to the phasor components so that the image resolution is not changed by the filter operation. The “average in cursor” button calculates the average phasor inside the pixels in the phasor plot covered by a cursor. The ‘color points’ and ‘white background’ tabs, when unchecked, change the image from color to grayscale and the phasor plot to a black background, respectively. ‘Masking’ and ‘save cursor’ checkmarks are explained later in the section of the protocol that deals with masking a part of the image to get the phasor information only from that region. The ‘plot histogram in 4 quadrants’ and ‘wavelength phasor’ buttons are related to the new spectral phasor technique wherein the spectral information from a point of an image is transformed to the phasor diagram. For spectral phasors there is no “universal circle” and the phasor values can span over the entire 360 degrees although the modulation is normalized so as not to exceed 1. ‘Number of columns’ and ‘zoom’ shows the number of images in one column and the size of each image, respectively. Box iv shows the name of the images

opened. The check sign next to the file name shows if they are being analyzed. If the check signs are unchecked then those samples are not analyzed and they are absent from the opened images and do not contribute to the phasor plot. Another possibility can be selected wherein the checkbox turns blue or gray. In this position the phasor images are shown but the phasor points calculated from these samples do not contribute to the cumulative phasor plot.

Supplemental Figure 2 box ii has seven tabs. The first tab 'cursor' is shown in Supplemental Figure 2a box (ii); 10 different cursors are available. Different color cursors can be selected using this tab and can be used to indicate a set of phasor points. The color of the cursor chosen can be modified by right clicking on the color and choosing from a color selection table. The size of cursor can be modified by changing the number (in pixel units) below the radius column. Supplemental Figure 2b represents the 'tau' tab. This tab can be used to calculate the phase and modulation lifetimes associated with a particular phasor selection or to resolve the exponential decay in components using two or more harmonics of the fluorescence decay. For, mono-exponential lifetimes the phase and modulation lifetimes are equal but for multi-exponential decays they differ. Supplemental Figure 2c shows the tab for 'formulas'. This tab can be used for the calculation and prediction of %FRET according to phasor approach. This tab is also used to calculate ion concentration, pK of indicators and Hill coefficients to calculate interactions using the Hill equation. If there is a change in fluorescence lifetime between bound and free species, this tab can be used to predict and calculate the aforementioned quantities. Supplemental Figure 2d shows the tab to change different parameters in the phasor plot. Among the various options 'show average lifetime' shows the average τ_P and τ_M on top of the phasor plot as selected by the cursor. The 'show label' option, when checked, shows the fraction of image covered by cursor 1, the total number of points above the threshold and the maximum intensity of that image, respectively, on top of that individual image. The different labels can be selected in the 'select labels' tab. The shape of the cursor can be modified using this tab. Four types of cursors, including circle, square, angular sector and inclined are available. The angular sector cursor is determined by the angle and width which determines the angle created with the (0,0) coordinate of the phasor plot and the broadness of the cursor, respectively. In the case of inclined cursor the angle and height determines the shape of the cursor. The zoom slider changes the scale of the phasor plot described in Supplemental Figure 2b. The scale increases when the cursor is moved toward the left. Supplemental Figure 2e depicts cursor linking. Using this tab, sets of two different cursors can be linked and mapped with the corresponding continuous color scheme. This operation is explained later. A right click on the color map opens a series of different color schemes and the links can be changed to any of these color schemes. Supplemental Figure 2f shows the tab for the statistics. The format of the statistics is the following: the image number, then fraction of area covered by a cursor and then the average intensity of the image covered. In this Supplemental Figure, the statistics page shows that for image 1, cursor 1 (usually red) covered 20.7% of the area with an average intensity of 5.3 counts/per image and cursor 2 covers 36% of the area and has an average intensity of 4.46 counts/image. This operation is repeated for the image 2 in the second line of the stats tab. The histogram to select a different intensities range for background correction or for looking above a certain range of intensities can be found in Supplemental Figure 2g. The zoom-in slider lets the operator select the background more carefully by extending to a lower intensity part of histogram.

Supplemental Figure 3 describes the internal tabs shown in the red box i of Supplemental Figure 2a. The options available are shown in Supplemental Figure 3a. The 'files' tab in Supplemental Figure 3b shows the option for open referenced files and various different saving options. One of the very important functions here is the save/load workspace option. This option lets one save all the details of one analysis including phasor positions, sizes, and color schemes and then, at a later time, reapply them to a different data set. This option allows one to repeat the same analysis pipeline for different data sets or to continue with the analysis if it has been stopped at a given point. 'Save ref files' gives an option to save masked ref files. Supplemental Figure 3c involves the 'assign' tab. This tab lets the operator chose different positions of the phasor plot for different species using separate cursors and then use the cursor positions to study and understand distributions of different species in the images. The 'tools' tab (Supplemental Figure 3d) is related to multiple different analysis schemes. Histograms of τ_P and τ_M calculate the distribution of phase and modulation lifetimes as selected by cursor 1. The next three formula buttons are related to calculation of pK, distribution between two species based on the linear additive properties of phasor and FRET, respectively, when they are used in conjunction with the assign tab. Once the positions are selected, the using 'assign' tab, memorizes the cursor positions to be used by buttons in 'tools' for the corresponding calculations. The 'show image' button transforms the image so that the average phasor positions from part of the image can be calculated. The next button, "show image in 3D", transforms the phasor color mapped image to a 3D plot where the height at each pixel (Z axis) is determined by the pixel intensity. This restriction lets one ascertain if there is a correlation of intensity changes with lifetime. The last part, including analysis of phasor distribution and the distance program, is related to calculation of differences between phasor distributions originating from two different types of samples and determination of how those differences can be maximized to create separation indexes. This approach has been explained elsewhere in much more detail[23]. The 'calculator' tab (Supplemental Figure 3e) is used for calculation of FRET using donor only lifetime and donor/acceptor lifetimes. When the high resolution button is checked, pressing the fractional intensity button results in a color heat map of the phasor points. The diffusion and log phasor plot are related to the diffusion phasor approach to calculate diffusion parameters at each pixel of an image. The concentration calibration part and use of distance and projection distance in 3 component analysis is described in further detail later in the manuscript. Finally, the "lifetime-form" window (Supplemental Figure 3f) can be accessed by pressing the 'lifetime form' button Supplemental Figure 3a. This window is used for opening files and converting to phasors, using Becker-Hickl card and Picoquant card and analysis using higher harmonics. This method can be also used for inserting a mask or calculation of average properties.

The basic color mapping using multiple cursor and continuous color schemes is shown in Supplemental Figure 4. Supplemental Figure 4a shows the intensity image and the appearance of the corresponding phasor plot for the autofluorescence of MEF cells. These images were background corrected using the intensity histogram shown in Supplemental Figure 2g. The intensity images were then converted to grayscale images by using the red box (iii) of Supplemental Figure 4a. Different populations of phasor points were then chosen using the red and green cursors and the grayscale images were color-mapped accordingly. One can see that the nucleus and cytoplasm have different FLIM signatures. Often a continuous distribution exists, resulting from mixing of species at the same pixel, and a two component

system is not sufficient to treat the data. This conclusion is evident from the empty areas of b. Thus a continuous color scheme is often used. Supplemental Figure 4c shows the continuous color scheme between two cursors and the corresponding phasor mapped FLIM images.

As mentioned before, the phasor map is a heat map of phasor points and the color of the phasor is dependent on the density of the phasor points at that particular phasor position. A high resolution image of this map (Supplemental Figure 5a) can be obtained by first clicking the 'high resolution' button and then pressing 'fractional intensity' (Supplemental Figure 5e). The actual 3D distribution (Supplemental Figure 5b) of the phasor points can then be obtained by clicking the 'show 3D' button in a. The 'tools' button in this 'fractional analysis' window (Supplemental Figure 5a) results in the options shown in c. These analyses schemes are described in detail later.

This part of this protocol paper gives an introduction to the FLIM module of the SimFCS software. The point by point methods to analyze FLIM data for multiple species, metabolism, and concentration calculations based on lifetime changes, masking, FRET and the reciprocity principle are described in more detail later. This part of the protocol is intended to give an introduction to various analysis methods available in SimFCS using the phasor approach to FLIM.